

# On the gap in the spectra of surface-layer atmospheric turbulence

V. Voronovich · G. Kiely

Received: 14 March 2006 / Accepted: 25 June 2006 /  
Published online: 12 December 2006  
© Springer Science+Business Media B.V. 2006

**Abstract** A large set of tower data was used to identify the gap that separates small-scale turbulence and mesoscale structures in the cospectra of surface fluxes. The cospectra were obtained using a multi-resolution decomposition algorithm. The gap time scale  $\tau_g$  was found by fitting a fifth-order polynomial to the cospectra and identifying special points occurring after the peak at small scales. In unstable conditions (day)  $\tau_g$  was found to fall as the mean wind speed increased, while no such dependence was observed in stable conditions (night). The gap scale was found to change very weakly with stability both in moderately stable and moderately unstable conditions, with a sharp drop from about 1100 to 250 s occurring in near-neutral conditions. The vertical fluxes computed at different averaging intervals were found to correlate exceptionally well with each other, the scatter being somewhat larger during the night. Although considerable discrepancy may occur for individual records, when averaged over 10 months, the difference in the flux estimated at 7 to 109 min intervals never exceeded 4%, which is comparable or less than the instrumental error.

**Keywords** Cospectral gap · Eddy covariance · Multi-resolution analysis · Surface fluxes

## 1 Introduction

In his famous paper Reynolds (1894) showed that turbulent fluxes of a property  $f$  can be measured by computing its covariance

$$\mathcal{F}_i = \overline{u'_i f'} \quad (1)$$

with the fluctuating components of wind velocity being  $u'_i$ . Here

---

V. Voronovich (✉) · G. Kiely  
Department of Civil and Environmental Engineering, University College Cork, Cork, Ireland  
e-mail: vvoronovich@phys.ucc.ie

$$u'_i = u_i - \bar{u}_i, \quad (2a)$$

$$f' = f - \bar{f}, \quad (2b)$$

and the overline is an averaging operation that must comply with a set of 'Reynolds averaging rules'. Ensemble, space and time averaging are all viable, but only the time average

$$\bar{f} = \frac{1}{\tau} \int_0^{\tau} f(t) dt \quad (3)$$

may be used when working with the data from a single tower.

Direct estimates of surface fluxes using eddy covariance (EC) use time series acquired by high-frequency instruments. The fluxes are computed according to (1) and (2), where

$$\bar{f} = \frac{1}{N} \sum_{j=0}^N f(j\Delta t), \quad (4)$$

and  $\Delta t$  is a sampling rate,  $N = \tau/\Delta t$  is the number of samples contained in the interval  $\tau$ . To employ the technique the appropriate time scale  $\tau$  for computing averages and covariances must be determined. The ergodic theorem states that time and ensemble averages coincide as  $\tau$  approaches infinity, provided the stochastic variable  $f(t)$  is stationary, i.e. its statistical moments do not change with time (e.g., Monin and Yaglom 1971). It would seem, then, that longer periods are needed in order to comply with the theorem, yet they cannot be too long, since the background state may cease to be stationary. The atmosphere evolves on a wide range of scales, from tenths of a second to years, and choosing a proper time scale to separate fluctuations from the mean is not at all trivial. When measurements are made over non-uniform terrain, the problem is further complicated by the necessity to rotate coordinates into the natural wind frame. The rotation introduces high-pass filtering, and therefore, may lead to an underestimation of vertical fluxes, if the averaging interval is too short (Finnigan et al. 2003; Finnigan 2004). In practice, periods from 30 min to 1 h are widely accepted (Panofsky and Dutton 1984; Kaimal and Finnigan 1994), although this choice is purely empirical, and no clear argument exists to support it.

The choice of the averaging period may not even be universal, but depend on the atmospheric conditions, site geometry or on the goal of the study. For example, researchers assessing the net ecosystem exchange (NEE) of trace gases are primarily interested in the total amount of the gas emitted by the plants to or extracted from the atmosphere, and therefore, may use longer averaging periods. Others, interested primarily in similarity relations, may choose a shorter one. Similarity theory assumes that the production and destruction of turbulence is 'local', i.e. depends only on the 'local' properties of the flow, such as wind shear or buoyancy. In reality the surface layer of the atmosphere contains both locally produced eddies and non-local, long scale structures, such as gravity waves, drainage flows, topographic circulations etc., usually referred to as 'mesoscale'. Typical time scales of the 'local' turbulence rarely exceed a few minutes, while transport at longer scales is mostly due to mesoscale structures. It is sporadic, not related to the local mean fields and does not obey the similarity theory (Smedman 1988). The result is a scatter in flux estimates and in displays of experimental data using similarity functions. To reduce scatter one needs

to average over the interval short enough to exclude transport by non-local structures (Mahrt et al. 2001).

Although the cospectra of small-scale turbulence and mesoscale structures are believed to overlap, often a gap separating them is observed, more likely so in stable conditions. At the gap scale  $\tau_g$  cospectra fall almost to zero after the peak at small scales associated with turbulence (see Fig. 1). Hence, a choice of  $\tau$  close to  $\tau_g$  may be ideal in order to separate local and non-local contributions into the surface fluxes (Mahrt et al. 2001; Vickers and Mahrt 2003).

The present study has two goals. The first is to check the occurrence of the gap in the cospectra of surface fluxes measured from the tower, to identify its typical time scale and to study its dependence on atmospheric conditions. The second is to assess the possibility of using shorter averaging intervals, close to  $\tau_g$ , in NEE studies. The site, the dataset, preliminary processing and filtering algorithms are described in Sect. 2. Our main tool for computation of turbulence spectra and cospectra, the multi-resolution analysis (MRA) (Howell and Mahrt 1997; Vickers and Mahrt 2003), is briefly described in Sect. 3, as well as the algorithm to identify the gap in the cospectra. Sect. 4 is devoted to dependencies of the gap scale on atmospheric conditions, namely, on stability and wind speed. Dependence of the vertical fluxes on the averaging period and the implications for NEE studies are described in Sect. 5. The results are briefly discussed in Sect. 6.

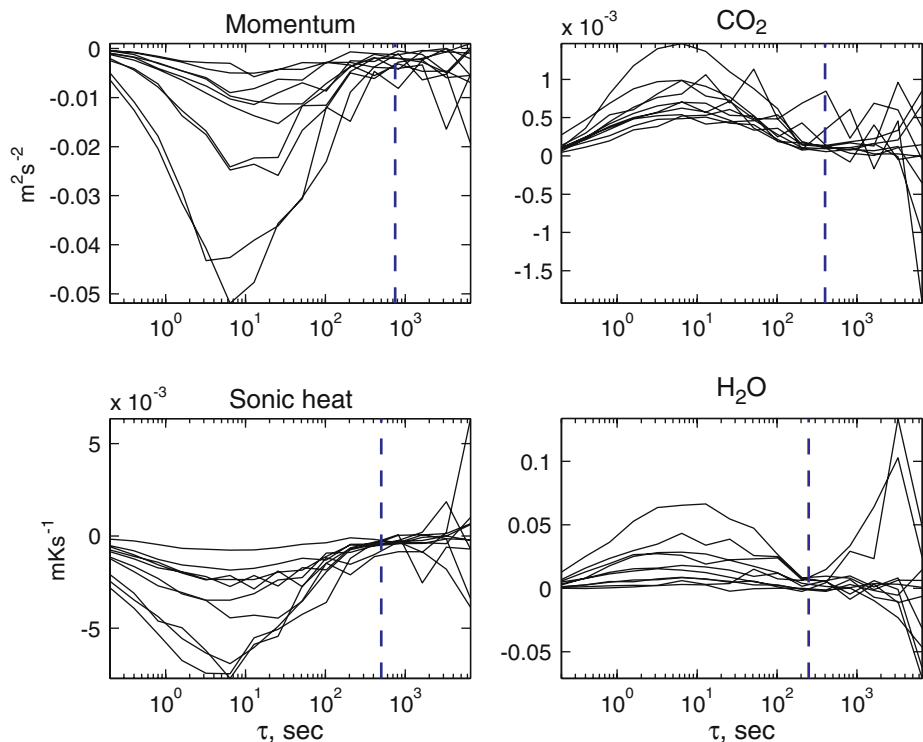


**Fig. 1** Sample cospectra of surface fluxes. Broken lines show approximate gap location

## 2 The data and preliminary processing

The data were acquired within the framework of CarboEurope–IP project and cover a 10-month period from March to December of 2004. The site is a managed, intensively grazed grassland in County Cork in southern Ireland (52.14°N; 8.66°W; 180 m above sea-level). The terrain is almost flat and mildly slopes south to north, where it meets a chain of small hills (50–100 m) approximately 2 km away from the tower. Wind speed and air virtual temperature were measured by a Gill Solent R3-50 sonic anemometer, CO<sub>2</sub> and water vapour concentrations by a LI-7500 infrared gas analyzer. Both devices were mounted on a tower at 3 m height over the ground and sampled at 10 Hz continuously.

The raw data underwent several stages of quality control and filtration. Records of  $N = 2^{16}$  points (duration  $T \simeq 109$  min) were created, as required by the multi-resolution decomposition algorithm (see, e.g., Howell and Mahrt 1997). These were overlapping, i.e. starting at  $2^{14}$  data points (27.3 min) one after the other, in order to increase the dataset and to better sample ever changing atmospheric conditions. Absolute values and spike filters were applied to instantaneous values of wind speed, temperature, CO<sub>2</sub> and H<sub>2</sub>O concentrations (Vickers and Mahrt 1997). Records missing more than 4% of points after filtering were discarded. The data within each record were rotated into the natural wind coordinate frame as described by Lee et al. (2004). Rotation completed, sonic heat flux  $\overline{w'\theta'}$ , friction velocity  $u_* = (-\overline{u'w'})^{\frac{1}{2}}$  and stability  $z/L$ , plus variance, skewness and kurtosis of the wind velocity components, temperature, CO<sub>2</sub> and H<sub>2</sub>O concentrations ( $c$  and  $q$ , respectively) were computed. Here  $z$  is the height of the instrument over the ground,

$$L = -\frac{u_*^3 \overline{\theta}}{\kappa g \overline{w'\theta'}} \quad (5)$$

is the Obukhov length and  $\kappa \simeq 0.4$  is von Karman's constant.

Statistical moments and variances were used for additional filtration of the data. Records were rejected, if

1. Skewness of  $u, v, w, \theta$  was outside the limits  $[-1; 1]$  or skewness of  $c, q$  was outside the limits  $[-1.5; 1.5]$ .
2. Kurtosis of  $u, v, w, \theta$  was outside the limits  $[2; 5]$  or kurtosis of  $c, q$  was outside the limits  $[1; 8]$ .
3. Values of pitch or roll angles, the ratios  $u_*/\bar{u}$  or  $(\overline{u'^2} + \overline{v'^2})^{\frac{1}{2}}/\bar{u}$ , variances of  $\theta, c$  or  $q$  were unreasonably high.

'Unreasonably high' values were found by computing the mean and the standard deviation of the parameters over the whole dataset and locating the records for which the values were more than three standard deviations away from the mean. These records were removed and the procedure repeated over the filtered dataset. 'Unreasonably high' values of the roll and pitch angles may happen due to failure of the rotation algorithm, which is not unusual in weak winds, or due to separation of the airflow from the underlying surface. In both cases vertical fluxes become contaminated by the horizontal component and the record should be discarded. The skewness/kurtosis filter is based on the assumption that atmospheric turbulence is statistically close to Gaussian noise (values of 0 and 3, respectively), and strong statistical deviations mainly result from malfunction of the instruments (Vickers and Mahrt 1997).

Additionally, the time series overlapping with the period of 1.25 h before/after sunset/dawn were excluded from further analysis to avoid instabilities due to rapid changes in the strength of solar radiation.

### 3 Multi-resolution decomposition and the cospectral gap

#### 3.1 Multi-resolution flux decomposition

Multi-resolution flux decomposition (MRFD) is a technique based on the Haar (Haar 1910), rather than Fourier, transform. Advantages of applying it to the analysis of turbulence spectra were discussed in detail by Howell and Mahrt (1997). It is enough to mention here that MRFD does not rely on any kind of periodicity in the recorded signal, which it decomposes locally; it does not violate Reynolds averaging rules; it is computationally less demanding and provides better resolution at small scales. There are several computer algorithms to perform multi-resolution decomposition, and we base ours on Vickers and Mahrt (2003).

Consider the time series of fluctuations (i.e. having zero mean) of some physical quantity  $f$  consisting of  $2^M$  points.

1. Divide the series in two and compute averages over the corresponding halves. This will result in the vector  $\mathbf{f}_M$  consisting of two components.
2. Subtract averages from the corresponding halves of the original time series.
3. Divide the resulting series into  $4 = 2^2$  subrecords of the length  $2^{M-2}$  and average to obtain a vector  $\mathbf{f}_{M-1}$  with four components.
4. Subtract averages from the corresponding quarters of the original time series.
5. Continue.

At step  $m$  of the process the series obtained from the previous step are divided into  $2^m$  sub-records of  $2^{M-m}$  points, and each sub-record is then averaged. This forms a vector  $\mathbf{f}_{M-m+1}$  consisting of  $2^m$  components. The averages are then subtracted from the corresponding parts of the whole series. The process is continued until step  $M$ , at which sub-records consist of one point only. The multi-resolution spectrum  $\hat{f}(j)$  of the variable  $f$  is then computed using

$$\hat{f}(j) = \frac{\mathbf{f}_j \cdot \mathbf{f}_j}{2^{M-j+1}}, \quad (6)$$

where ‘ $\cdot$ ’ denotes the classical dot-product of two vectors. Given the second variable,  $g$ , the cospectrum can be computed in the same manner

$$\hat{f}_g(j) = \frac{\mathbf{f}_j \cdot \mathbf{g}_j}{2^{M-j+1}}. \quad (7)$$

An attractive property of multi-resolution cospectra is the ease of their interpretation. Each value  $\hat{f}_g(j)$  in (7) is just the contribution to the total transport from the turbulent structures with the scales ranging from  $2^{j-1} \Delta t$  to  $2^j \Delta t$ . The total covariance, as computed by averaging over  $\tau_j = 2^j \Delta t$ , can be obtained from the multi-resolution cospectrum by simple summation

$$\mathcal{F}_g[\tau_j] = \sum_1^j \hat{f}_g(k). \quad (8)$$

### 3.2 Cospectral gap

Sample multi-resolution cospectra of the surface fluxes computed from several nighttime records are shown in Fig. 1. The gap, separating small-scale turbulence and mesoscale motions, is clearly visible in the region of 300–800 s, where the cospectra fall almost to zero after the peak associated with the turbulence. In this region the corresponding total fluxes, which are the integrals of the cospectra, change very little with the averaging interval. Hence, the uncertainty in the eddy-covariance flux estimate should be smallest once the averaging period is chosen close to  $\tau_g$ . Consider also that in the turbulence region (time scales smaller than 400 s) all spectral components have the same sign, depending on the stability, whereas at large scales the cospectra are highly erratic. Even the signs may be different for the neighbouring spectral components. This erratic behaviour is exactly the reason why mesoscale motions are so poorly described by any kind of similarity theory.

Multi-resolution analysis completed, one needs to identify the numerical value of  $\tau_g$  from the cospectra and, preferably, to do this automatically for each of the 109-min records. Unfortunately, it is extremely difficult, if possible at all, to build a robust procedure for this purpose. Even when the gap, normally associated with the minimum in the cospectrum, is present, the cospectral curves tend to be highly irregular, with a number of local extrema, which result from random noise and can mislead the automatic algorithm. To bypass this problem some authors processed the cospectra with a 1-2-1 smoothing filter prior to the search for minima (Vickers and Mahrt 1997), which does remove a number of auxiliary extrema and makes the gap much easier to identify. Attractive as this may appear, application of smoothing filters based on the running average (1-2-1 is essentially a weighted running average) to turbulence data is questionable, as this operation does not satisfy Reynolds rules (Kaimal and Finnigan 1994). An alternative is to define  $\tau_g$  for a longer time period, such as the whole night or day, i.e. on the basis of several individual 2-h time series (Howell and Sun 1999; Morales et al. 2004), to decrease the error due to better sampling. The latter approach suited well the purposes of the studies cited above, but is not of much use for the present one, with the gap itself being its main goal. The atmosphere is not stationary over long periods, and the gap scale can change significantly throughout the day or night, especially during sunset/dawn transitions.

One problem associated with the orthogonal Haar transform is that its resolution decreases at large scales. Indeed, the spectrum is estimated at a finite, and usually small, number of points (16 in our case), with the basic periods differing by a factor of two. To improve the accuracy and to facilitate identification of the gap in an unattended regime we used the following approach. A low-order polynomial  $P(\tau)$  was fitted by a least squares technique to each individual cospectrum  $\hat{f}_g(j)$ . The fit was deemed unsuccessful, if the error

$$\mathcal{E} = \frac{\sum_1^M [P(j) - \hat{f}_g(j)]^2}{\sum_1^M [\hat{f}_g(j) - \langle \hat{f}_g \rangle]^2} \quad (9)$$

exceeded a prescribed value. Here  $M$  is the number of the Haar functions in the basis and  $\langle \hat{f}_g \rangle$  the average value of the cospectrum

$$\langle \hat{f}_g \rangle = \frac{1}{M} \sum_1^M \hat{f}_g(j).$$

The fit completed,  $\tau_g$  was defined by the special points of the polynomial with the following algorithm (see Fig. 2)

1. The polynomial was checked for an extremum in the turbulence region, at  $\tau = E_0 < 400$  s.
2. The polynomial was checked for roots,  $R_i$ , extrema,  $E_i$  and inflection points,  $I_i$ , at  $E_0 < \tau < T$  (here  $I_1 < I_2 < \dots$ ).
3. The derivative at  $\tau = I_2$  was checked to be small

$$|P'(I_2)/P'(I_1)| < 1/2.$$

4. The gap time scale was found from

$$P(\tau_g) = P(\tau_m) + 0.02(P(E_0) - P(\tau_m)) \tag{10}$$

where  $\tau_m = \min \{E_1, R_1, I_2\}$

Whether the gap scale is defined by  $E_1, R_1$  or  $I_2$  depends on the particular scenario of transport. In the first case turbulence and mesoscale structures transport in the same direction. In the second, the transport direction changes at the scale  $\tau = R_1 < T$ , and one would observe a maximum in the total flux as a function of  $\tau$ . In the last case the spectrum does change its sign, but at the scale  $\tau > T$  that cannot be resolved. Nevertheless, an inflection point  $I_2$  indicates a plateau in the spectral curve and may be accepted as the gap scale, provided  $P'(I_2)$  is small.

Two major problems encountered were the inability to achieve a polynomial fit with the required goodness and the absence of extrema, roots or inflection points of the polynomial at  $E_0 < \tau < T$ . The latter problem was expected, since the spectra of turbulence and mesoscale motions do not always separate and the gap may simply

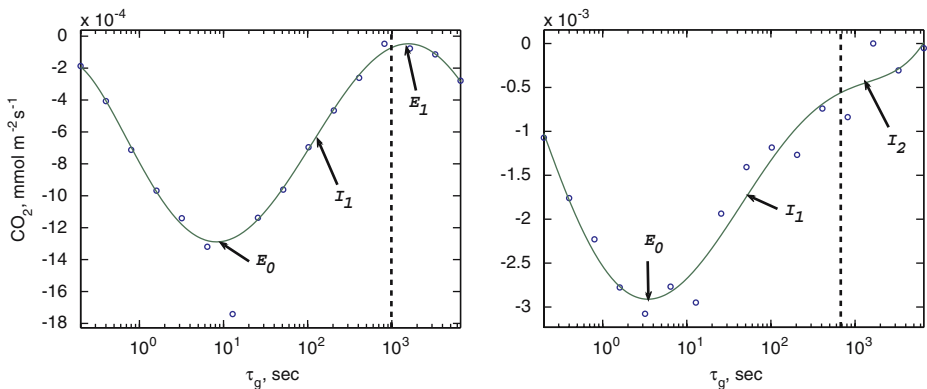


**Fig. 2** Gap time scale identification by fitting a fifth-order polynomial (solid line) to data (circles). Broken lines are drawn at the gap scale

**Table 1** Percentage of successful polynomial fits to different spectra and cospectra versus the prescribed margin of error and the order of the polynomial

| $N$               | 4             |       |       |       | 5     |       |       |       |
|-------------------|---------------|-------|-------|-------|-------|-------|-------|-------|
|                   | $\mathcal{E}$ | 0.15  | 0.2   | 0.25  | 0.3   | 0.15  | 0.2   | 0.25  |
| $\overline{u'w'}$ | 0.040         | 0.167 | 0.376 | 0.588 | 0.222 | 0.461 | 0.646 | 0.730 |
| $\overline{w'T'}$ | 0.010         | 0.348 | 0.609 | 0.786 | 0.381 | 0.638 | 0.788 | 0.844 |
| $\overline{w'C'}$ | 0.094         | 0.308 | 0.569 | 0.716 | 0.315 | 0.577 | 0.723 | 0.786 |
| $\overline{w'H'}$ | 0.110         | 0.345 | 0.592 | 0.741 | 0.342 | 0.603 | 0.721 | 0.780 |
| $\overline{u'^2}$ | 0.031         | 0.089 | 0.164 | 0.240 | 0.069 | 0.160 | 0.253 | 0.320 |
| $\overline{v'^2}$ | 0.019         | 0.044 | 0.091 | 0.154 | 0.052 | 0.122 | 0.192 | 0.240 |
| $\overline{w'^2}$ | 0.894         | 0.972 | 0.988 | 0.991 | 0.979 | 0.989 | 0.990 | 0.991 |
| $\overline{T'^2}$ | 0.066         | 0.162 | 0.242 | 0.283 | 0.192 | 0.280 | 0.346 | 0.375 |

not exist. The former is due to the highly erratic nature of turbulence data. Imagine the series, which has the value +1 at odd points and -1 at even. An attempt to fit such data by *any* kind of function with  $\mathcal{E} < 1$  is doomed to failure. Table 1 shows the success rate of fitting cospectra of surface fluxes and spectra of variances of wind speed and temperature by polynomials of order  $\mathcal{N} = 4$  and 5. The success rate depends on  $\mathcal{E}$ ,  $\mathcal{N}$  and on the flux/variance in question. Higher values of  $\mathcal{N}$  cannot be used since the polynomial tends to reproduce the erratic behaviour of the data already at  $\mathcal{N} = 6$ . Note that the success rate is much lower than average for  $\overline{u'^2}$ ,  $\overline{v'^2}$  and  $\overline{\theta'^2}$ , whereas for  $\overline{w'^2}$  it is extraordinarily high. In contrast to scalars, velocity components are affected also by pressure forces, poorly accounted for by existing theories. Temperature is not completely a passive scalar, the spectrum of its variance is closely related to that of the active turbulence fields, i.e. of wind velocity. The momentum flux is more difficult to treat than others, probably, due to the same reasons.

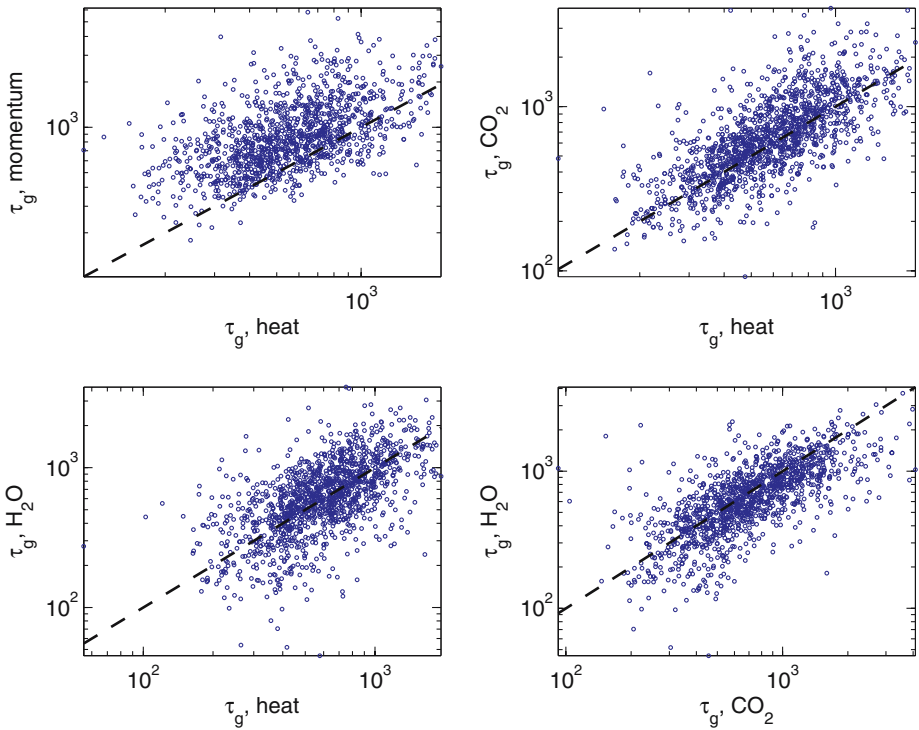
Time scales of the gap in the cospectra of different fluxes are reasonably close to each other, with the exception of momentum flux, with  $\tau_g[\overline{u'w'}]$  being approximately 40% higher than, say,  $\tau_g[\overline{w'\theta'}]$ , see Fig. 3. A possible explanation could be the tendency of turbulent eddies to elongate in the streamwise direction, especially in strong winds, or the effect of pressure forces mentioned above.

Table 2 shows the value of  $\tau_g$  averaged over all daytime records as a function of  $\mathcal{E}$  and  $\mathcal{N}$ . For the majority of the fluxes/variances the difference in the values of  $\tau_g$  computed with  $\mathcal{E} = 0.15$  and with  $\mathcal{E} = 0.3$  does not exceed 10%.<sup>1</sup> Dependence on the order of the polynomial is stronger, but does somewhat saturate with its growth, i.e. the relative difference in the values of  $\tau_g$  obtained with the polynomial fits of orders  $\mathcal{N}$  and  $\mathcal{N} + 1$  decreases, as  $\mathcal{N}$  grows. Hereinafter, we adopt  $\mathcal{E} = 0.25$  and  $\mathcal{N} = 5$  for all calculations.

#### 4 Dependence of the gap scale on environmental conditions

Assuming that the spectra of small-scale turbulence and mesoscale structures do separate, the gap time scale should be roughly equal to the largest period of turbulent

<sup>1</sup> The difference is much larger for  $\tau_g[\overline{T'^2}]$  and  $\tau_g[\overline{v'^2}]$ , but this is mainly due to the fact that the success rate is so low for  $\mathcal{E} = 0.15$ ,  $\mathcal{N} = 4, 5$ .



**Fig. 3** Correlation of gap time scales in the cospectra of different vertical fluxes. Broken lines are 100% correlation

**Table 2** Average gap time scale (seconds) in the cospectra of daytime fluxes and velocity spectra versus the error  $\mathcal{E}$  and the order of the polynomial  $N$

| $N$               | 4    |      | 5    |      | 6    |      |
|-------------------|------|------|------|------|------|------|
| $\mathcal{E}$     | 0.15 | 0.3  | 0.15 | 0.3  | 0.15 | 0.3  |
| $\overline{u'w'}$ | 1551 | 1460 | 1067 | 1194 | 959  | 1076 |
| $\overline{w'T'}$ | 846  | 924  | 716  | 743  | 672  | 673  |
| $\overline{w'C'}$ | 1140 | 1156 | 892  | 920  | 823  | 837  |
| $\overline{w'H'}$ | 1060 | 1130 | 825  | 859  | 778  | 802  |
| $\overline{u'^2}$ | 2872 | 2848 | 2614 | 2692 | 2132 | 2253 |
| $\overline{v'^2}$ | 2925 | 2832 | 1905 | 2640 | 1753 | 2201 |
| $\overline{w'^2}$ | 452  | 491  | 344  | 346  | 391  | 390  |
| $\overline{T'^2}$ | 621  | 956  | 542  | 854  | 700  | 858  |

motion, and, hence, proportional to the size of the largest locally-produced eddies. Primary sources/sinks of atmospheric turbulence are wind shear and buoyancy, hence, one would expect some relationship between  $\tau_g$  and these parameters. Wind shear roughly defines the vertical scale of the eddies that extract energy from the mean flow, and this has to be close to their maximal size, as the cascade mechanism can only transfer energy to smaller scales (Tennekes and Lumley 1972). According to

Monin–Obukhov similarity theory, the local value of the wind shear scales with friction velocity  $u_*$  and stability  $z/L$ , and so should the gap scale. If stratification is stable, buoyancy tends to destroy turbulent eddies, in particular those with the spatial scale exceeding the Obukhov length. Hence, dependence of  $\tau_g$  on  $L$  in stable conditions is expected.

Vickers and Mahrt (2003) have shown that the gap time scale decreases as stability grows and increases with the height of the instrument over the ground. The former dependence is verified by the present study, as Fig. 4 indicates, although the scatter is so large that no functional fit is possible. The broken line in the figure shows the bin averaged value obtained by the following algorithm. Starting from the smallest value of stability encountered in the data, the size of the bin was increased by 0.03 until at least 25 data points were in the bin. Once this was achieved the next bin was constructed starting from the upper border of the previous. This technique was aimed at avoiding statistical deviations by ensuring that the number of points in each of the bins is not too small. The results are somewhat similar to those of Vickers and Mahrt (2003): the gap scale changes very little in moderately stable/unstable conditions, with a large fall as the stability changes sign, i.e. in the near-neutral region.

Figure 5 shows the time scale of the gap in the cospectra of surface fluxes and the spectrum of vertical velocity as a function of the mean wind speed  $\langle u \rangle$ , daytime records. Dependence on the friction velocity  $u_*$  is very similar, since it is strongly correlated with  $\langle u \rangle$ , especially in neutral and weakly stable/unstable conditions that

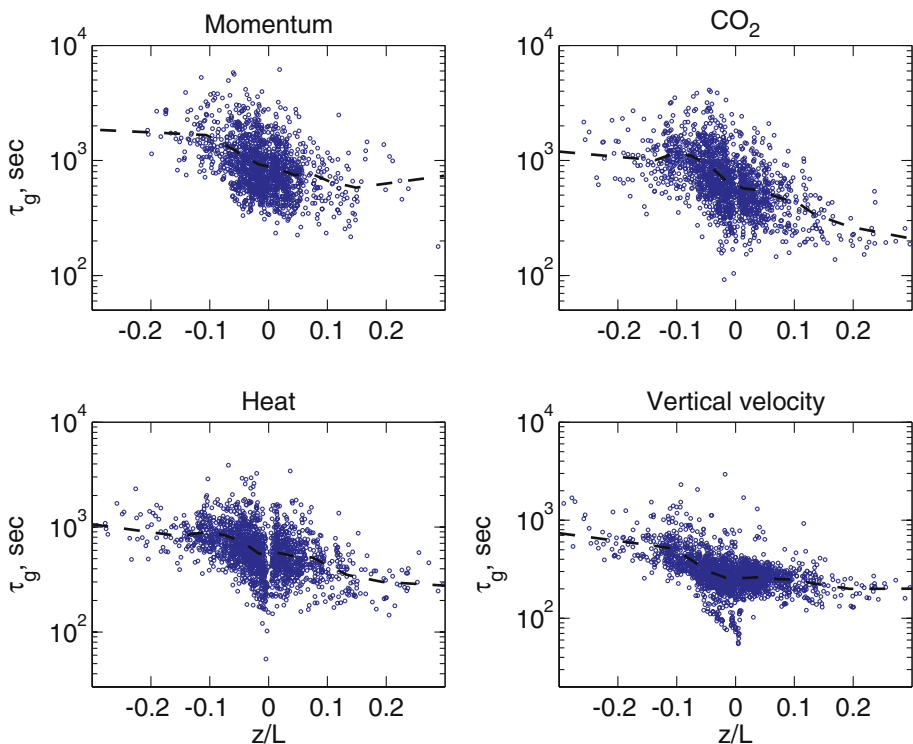


**Fig. 4** Gap time scale vs stability  $z/L$ . Broken lines correspond to bin-averaged values

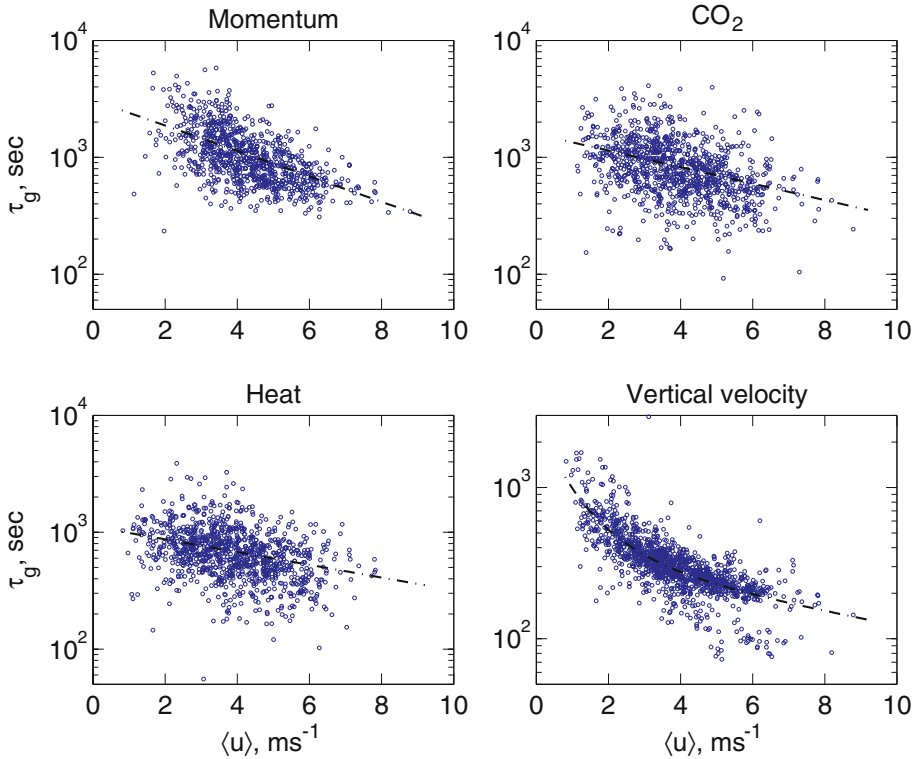


**Fig. 5** Gap time scale versus mean wind speed, daytime records. Broken line is  $\log_2 \tau_g = a \exp\{b\langle u \rangle\} + c \exp\{d\langle u \rangle\}$  in the lower right panel, and  $\tau_g = a \exp\{b\langle u \rangle\}$  in the other panels

were most common during the study. Broken lines in all panels except the lower right correspond to a simple exponential fit  $\tau_g = a \exp\{b\langle u \rangle\}$ , whereas at the latter the broken line is given by

$$\log_2 \left( \tau_g \left[ \overline{w^2} \right] \right) = a \exp\{b\langle u \rangle\} + c \exp\{d\langle u \rangle\},$$

i.e. it is  $\log_2(\tau_g \overline{w^2})$  that is fitted well by two exponential functions. Exact values of the coefficients of the fits are not of importance at this stage, as the scatter in the values of  $\tau_g$  is very large. Nevertheless, the fit does show clearly that  $\tau_g$  reduces from approximately 1300 to 400 s (2400 to 400 s for the momentum flux, and 1000 to 130 s for vertical velocity) as the wind speed increases from 1 to 9 m s<sup>-1</sup>. The height of the instrument over the ground being fixed, an increase in the wind speed indicates an increase in the wind shear, and, by the argument above, a decrease in the size and time scale of the night extracting eddies.

Surprisingly, at night any dependence of  $\tau_g$  on the wind speed seems to be absent, except for the vertical velocity (see Fig. 6). Nighttime values of  $\tau_g$  are in the range 400–500 s for heat and CO<sub>2</sub> fluxes, 700–900 s for momentum, and change very little with the wind speed. Apparently, in stable conditions normally met at night,  $\tau_g$  is controlled by stratification, i.e.  $L$ , rather than wind shear. This fact is implicitly corroborated by a slight increase in the values of  $\tau_g$  with the wind speed observed at

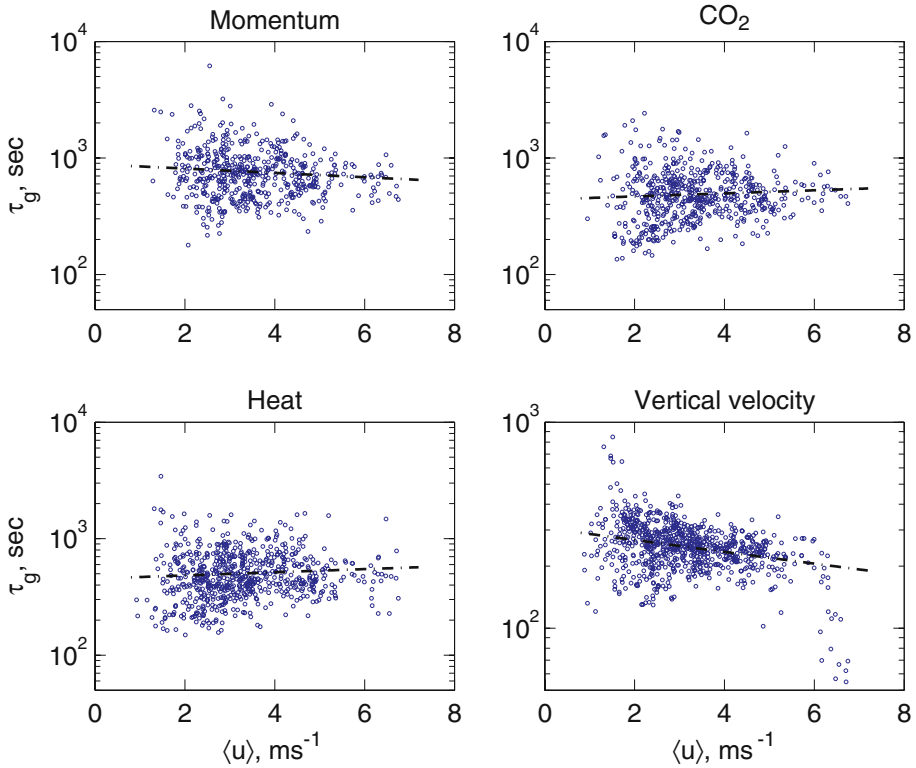


**Fig. 6** Gap time scale versus mean wind speed, nighttime records. Broken lines are exponential fits:  $\tau_g = a \exp\{b\langle u \rangle\}$

night (see Fig. 6, heat and  $\text{CO}_2$  fluxes). Consider that due to high correlation with the friction velocity larger values of  $\langle u \rangle$  tend to correspond to smaller values of stability, and thus, according to Fig. 4, to larger values of  $\tau_g$ .

In contrast to surface fluxes,  $\tau_g[\overline{w'^2}]$  does decrease with the wind speed at night (stable conditions), from around 300 to just 190 s in high winds, the dependence being well fitted by a simple exponential.

## 5 Eddy-covariance flux estimates and averaging interval

Vertical fluxes, as estimated by the eddy-covariance technique, clearly depend on the averaging interval. The structures evolving at time scales larger than  $\tau$  are not distinguishable from the stationary fields and do not contribute to the total flux. Rotation into the natural wind frame, performed at every averaging period, introduces additional high-pass filtering (Finnigan et al. 2003; Finnigan 2004). As a result there is an ongoing argument in favour of increasing the values of  $\tau$  in order to avoid ‘flux loss’. Yet, a closer look at Fig. 1 leads to just the opposite conclusion. The cospectra at large scales are highly erratic, their amplitude and even the sign change from point to point and from record to record. This behaviour may result in the huge scatter in

flux estimates and even in non-physical and countergradient values, if long averaging intervals are used. For example, the cospectra shown in Fig. 1 are all from nighttime records, when the  $\text{CO}_2$  flux is expected to be positive (production/source), and so are *all* spectral components at small scales. Yet, at longer scales (30 min to 1 h) some are negative (consumption/sink). Obviously, to obtain physically meaningful results one has to filter these out, i.e. to use shorter averaging intervals.

Another reason for uncertainty at large scales is insufficient sampling. Consider that in our case estimates of the flux at all scales are obtained from one master record of  $T = 109$  min duration. However, the flux estimate at  $\tau = T$  involves only one sub-record, whereas at  $\tau = T/n$  it is obtained by averaging over  $n$  non-overlapping sub-records. A random flux sampling error can be defined as

$$\epsilon = \frac{\sigma_f}{n^{1/2}} \quad (11)$$

where  $\sigma_f$  is the square root of the variance of the flux between the sub-records (Mahrt 1998; Howell and Sun 1999). The error clearly decreases as the number  $n$  grows, and that is why the cospectra appear much more regular at small scales. In a way, dividing the original record into sub-records and averaging the flux estimates obtained from the latter is similar to using repeated passes, when measuring fluxes from the aircraft (Mahrt 1998).

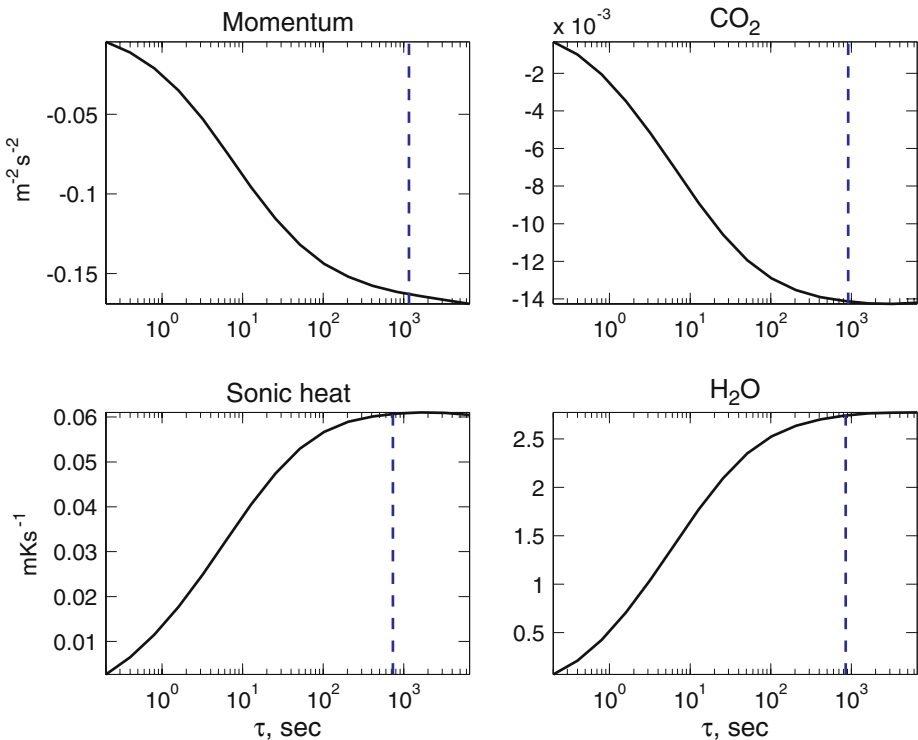


**Fig. 7** Ogive curves of surface fluxes averaged over all daytime records. Broken lines are drawn at the average gap time scale

The fear that using shorter averaging periods will result in ‘flux loss’ and an inability to close the energy balance may not be justified. In studies such as CarboEurope-IP the primary interest is not in the individual flux estimates, but in the annual balances of heat, water vapour or trace gases. One may wonder, then, how the annual budgets depend on the averaging interval adopted for the study? Multi-resolution decomposition provides the means to assess this problem. The dependence of the total flux on the averaging interval can be easily obtained with the help of Eq. 8, the resulting curve being called the ogive (Lee et al. 2004). Figure 7 shows the ogives of the surface fluxes averaged through all 10 months of daytime records. It is clear that  $\text{CO}_2$  and humidity fluxes reach their asymptotic values at the time scale of approximately 800–900 s, rather than at 1 h or even 30 min. The ogive of the heat flux actually reaches a maximum at  $\tau=16$  min, which means that it may be underestimated by using  $\tau=30$  min as the averaging interval. Long-scale transport may be large for each individual record, but its effect averages almost to zero over the year due to its sporadic nature and better sampling. The only property effectively transported at long scales is momentum, and its ogive does not reach a horizontal asymptote even at 109 min.

Averaged ogives for the night periods are plotted in Fig. 8. Now only the humidity flux does reach the maximum at  $\tau \simeq 15$  min, but neither of the other three comes close to asymptotic behaviour. This fact is counterintuitive, as the values of  $\tau_g$  were found to be much smaller at night, and one would expect the ogives to level at  $\tau \simeq \tau_g$ . Probably, mesoscale structures are much less erratic at night (stable conditions), since

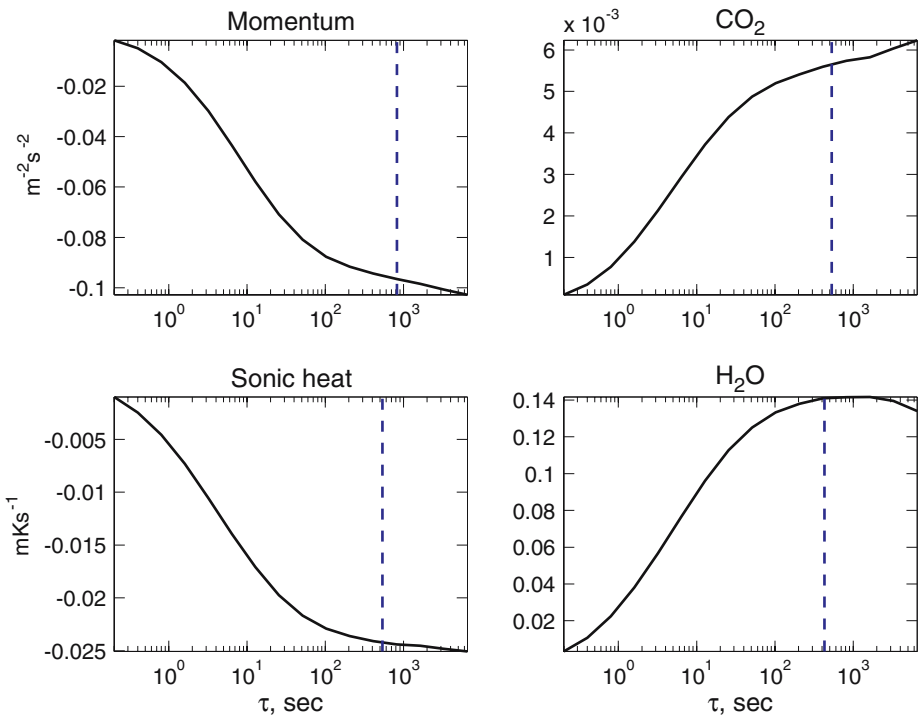


**Fig. 8** Ogive curves of surface fluxes averaged over all nighttime records. Broken lines are drawn at the average gap time scale

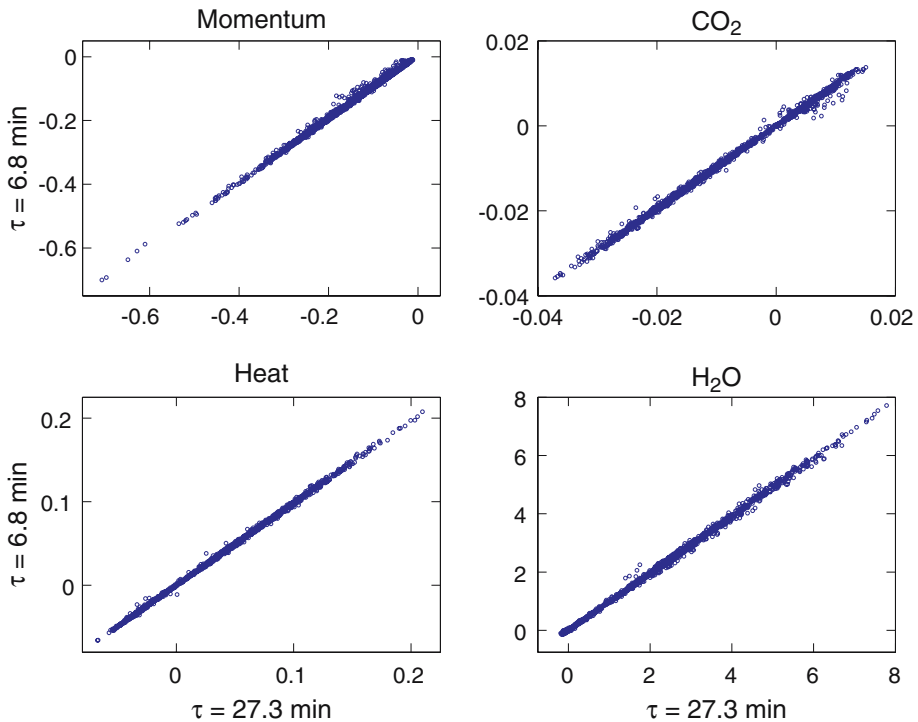


**Fig. 9** Fluxes at 6.8 min averaging interval vs fluxes at 27.3 min

their annual input into the total flux is non-zero. This is certainly true for gravity waves, which possess a high degree of regularity. Moreover, one could argue that mesoscale structures are likely to be relatively more important at night since the total flux is less, and wave activity, drainage flows, and the effects of terrain heterogeneity are larger.

In Fig. 9 fluxes (both daytime and nighttime records) estimated at  $\tau=6.8$  min are plotted against those estimated at  $\tau=27.3$  min. The slopes of the best linear fits,  $y = \alpha x + \beta$ , range from 0.97 for CO<sub>2</sub> to 0.99 for the momentum flux, with  $|\beta| < 0.004$  for all fluxes. The same exercise performed at  $\tau=6.8$  min and  $\tau=109$  min yields slopes of 0.96–0.99 and  $|\beta| < 0.008$ . In other words, the average error in the flux estimate resulting from the choice of  $\tau$  is less than 4% for all fluxes, both during the day and night. Considering that instrumentation, filtration and processing errors are, probably, larger than this value (Baldocchi 2003), it does seem that using averaging intervals as short as 7 min would not affect annual budgets of heat, CO<sub>2</sub> or water.

## 6 Conclusions

A large set of tower data was used to study the gap in the cospectra of surface fluxes and the spectra of vertical velocity. The cospectra were obtained by using the multi-resolution decomposition algorithm based on the Haar transform. The gap time scale,  $\tau_g$ , was found by fitting a fifth-order polynomial to a cospectrum and studying its special points. The gap was successfully identified in approximately 75% of the records,

both during the day and night, in both high and low winds, and in both stable and unstable conditions. Numerical values of  $\tau_g$  derived from the cospectra of scalar fluxes are close to each other, while for the momentum flux they are about 40% larger.

In unstable conditions (day)  $\tau_g$  decreases with the wind speed, the variation comparatively well fitted by an exponential function. The wind speed,  $\bar{u}$ , rather than the Obukhov length,  $L$ , seems to be the controlling parameter for the gap time scale in the unstable atmosphere. On the contrary, no dependence of  $\tau_g$  on  $\bar{u}$  was discovered in stable conditions (night). Stratification has a much more pronounced effect on the turbulence properties than does the wind shear, i.e. stability,  $z/L$ , rather than  $\bar{u}$ , is the governing parameter at night. Dependence of  $\tau_g$  on  $z/L$  was found by the adaptive bin averaging technique. The gap time scale changes very little in moderately stable/unstable conditions, with a large decrease in near-neutral conditions as  $z/L$  increases.

Spectra of vertical velocity are much more regular and less contaminated by meso-scale structures than are cospectra of surface fluxes. The gap is pronounced and easily identifiable, and the success rate of the gap finding algorithm is extremely high (up to 99%). Typical values of  $\tau_g[\overline{w'^2}]$  are considerably and consistently smaller and much less scattered than the values of  $\tau_g[\overline{w'T'}]$ , for example. Finally, the functional dependence of  $\tau_g[\overline{w'^2}]$  on the wind speed is qualitatively different. At night (stable conditions) it does fall with the mean wind speed, the dependence being well fitted by an exponential. During the day (unstable atmosphere)  $\tau_g$  falls with  $\bar{u}$  as well, but it is  $\log_2(\tau_g[\overline{w'^2}])$  that is well fitted by the double exponential. Apparently, fluctuations of the vertical velocity are much more sensitive to changes in the wind speed than are the surface fluxes.

Our study has shown that the fluxes computed at different averaging intervals correlate exceptionally well with each other. Although changing  $\tau$  from 6.8 to 109 min may result in considerable discrepancy of the flux estimates for individual records, when averaged over 10 months, the fluxes differ by less than 4% from the values obtained at a 27.3 min period. This is comparable or less than the instrumental error and may safely be neglected. Long-scale transport, though significant for individual records, averages almost to zero over the year due to its sporadic nature and does not affect the annual balance of heat, CO<sub>2</sub> or water vapour transferred between the surface and the atmosphere. At the same time, using shorter averaging intervals or even an adaptive averaging at the gap scale, is expected to reduce the scatter in the flux estimates and similarity relations, once the mesoscale transport is excluded.

An ideal strategy for EC flux estimates may be recording comparatively long time series, of order of 1–2 h, rotating the variables at the long scale to avoid high-pass filtering, applying multi-resolution decomposition and, finally, evaluating the fluxes at the scale close to that of the cospectral gap. An additional advantage is considerably improved sampling and expected reduction of the scatter due to the averaging of short-term flux values over the whole record. Howell and Sun (1999) and Vickers and Mahrt (2003) clearly show how the sampling error is reduced in the process.

However, further studies for different ecosystems, terrain, and, especially, in different climates (dry/humid) are needed to verify our results.

**Acknowledgements** This work is part of the Environmental Research Technological Development and Innovation program, managed by the Irish EPA and financed by the Irish Government under the National Development Plan 2000–2006 (CELTICFLUX, 2001-CC-C2-M1). The European Union CARBOEUROPE-IP program funds the first author. Adrian Birkby provided essential instrumentation and data collection support for this research.

## References

- Baldocchi DD (2003) Assessing the eddy covariance technique for evaluating carbon dioxide exchange rates of ecosystems: past, present and future. *Global Change Biol* 9:479–492
- Finnigan JJ, Clement R, Malhi Y, Leuning R, Cleugh HA (2003) A re-evaluation of long-term flux measurement techniques Part I: averaging and coordinate rotation. *Boundary-Layer Meteorol* 107:1–48
- Finnigan JJ (2004) A re-evaluation of long-term flux measurement techniques Part II: coordinate systems. *Boundary-Layer Meteorol* 113:1–41
- Garratt JR (1992) *The atmospheric boundary layer*. Cambridge University Press, UK, 316 pp
- Haar A (1910) Zur theorie der orthogonalen funktionensysteme. *Math Ann* 69:331–371
- Howell JF, Mahrt L (1997) Multiresolution flux decomposition. *Boundary-Layer Meteorol* 83:117–137
- Howell JF, Sun J (1999) Surface-layer fluxes in stable conditions. *Boundary-Layer Meteorol* 90:495–520
- Kaimal JC, Finnigan JJ (1994) *Atmospheric boundary layers: their structure and management*. Oxford University Press, New York, 289 pp
- Lee X, Finnigan J, Paw UKT (2004) Coordinate systems and flux bias errors. In: Lee X, Massman W, Law B (eds) *Handbook of micrometeorology: a guide for surface flux measurements*. Kluwer Academic Publishers, pp 33–67
- Mahrt L (1998) Flux sampling errors for aircraft and towers. *J Atmos Oceanic Tech* 15:416–429
- Mahrt L, Moore E, Vickers D, Jensen NO (2001) Dependence of turbulent velocity variances on scale and stability. *J Appl Meteorol* 40:628–641
- Monin AS, Yaglom AM (1971) *Statistical fluid mechanics: mechanics of turbulence*, Vol. 1. MIT Press, Cambridge (MA), 640 pp
- Morales OLL, Acevedo OC, da Silva R, Magnaco R, Siqueira AC (2004) Nocturnal surface-layer characteristics at the bottom of a valley. *Boundary-Layer Meteorol* 112:159–177
- Panofsky HA, Dutton JA (1984) *Atmospheric turbulence: models and methods for engineering applications*. John Wiley & Sons Inc., New York, 418 pp
- Reynolds O (1894) On the dynamical theory of incompressible viscous fluids and the determination of the criterion. *Phil Trans R Soc London* 186:123–161
- Smedman AS (1988) Observations of a multi-level turbulence structure in a very stable atmospheric boundary layer. *Boundary-Layer Meteorol* 44:231–253
- Tennekes H, Lumley JL (1972) *A first course in turbulence*. The MIT Press, MA, 313 pp
- Vickers D, Mahrt L (1997) Quality control and flux sampling problems for tower and aircraft data. *J Atmos Oceanic Tech* 14:512–526
- Vickers D, Mahrt L (2003) The cospectral gap and turbulent flux calculations. *J Atmos Oceanic Tech* 20:660–672